Structure and dielectric characterization of the $La(Mg_{1/2}Ti_{1/2})O_3$–$Nd(Mg_{1/2}Ti_{1/2})O_3$ system

2003 J. Phys.: Condens. Matter 15 4229

(http://iopscience.iop.org/0953-8984/15/24/316)

INSTITUTE OF PHYSICS PUBLISHING JOURNAL OF PHYSICS: CONDENSED MATTER

J. Phys.: Condens. Matter **15** (2003) 4229–4238 PII: S0953-8984(03)60562-X

Structure and dielectric characterization of the $La(Mg_{1/2}Ti_{1/2})O_3$–$Nd(Mg_{1/2}Ti_{1/2})O_3$ system

M P Seabra, A N Salak[1], M Avdeev and V M Ferreira

Department of Ceramic and Glass Engineering/CICECO, University of Aveiro, 3810-193 Aveiro, Portugal

E-mail: salak@cv.ua.pt

Received 6 March 2003
Published 6 June 2003
Online at stacks.iop.org/JPhysCM/15/4229

Abstract

$(1-x)La(Mg_{1/2}Ti_{1/2})O_3$–$xNd(Mg_{1/2}Ti_{1/2})O_3$ $[0 \leqslant x \leqslant 1]$ ceramics were prepared from powders obtained by a non-conventional chemical route based on the Pechini method. $La(Mg_{1/2}Ti_{1/2})O_3$ and $Nd(Mg_{1/2}Ti_{1/2})O_3$ were found to form perovskite solid solutions in the whole compositional range. The structure of all the compositions was refined using the $P2_1/n$ space group, which allows account of B-site ordering. The relative permittivity and temperature coefficient of the resonant frequency measured in the gigahertz range were analysed with respect to composition of the system. The non-monotonic dependence of the microwave quality factor on x was described qualitatively with the damped classical oscillator model and assuming 'two-mode' behaviour of the $A \leftrightarrow BO_6$ vibration mode in the solid solutions.

1. Introduction

Rapid growth of the microwave communication system has stimulated a search for new effective low-cost materials for applications such as resonators and filters. The requirements for these materials are high dielectric permittivity (ε') and quality factor (Q) as well as a close to zero value of temperature coefficient of the resonant frequency (τ_f) [1]. However, their nature is interrelated and an attempt to improve one of the parameters commonly leads to worsening the others. Therefore, the task to satisfy all the conditions is mainly to find the best compromise. A class of perovskite-related non-ferroelectric materials is known to be appropriate for microwave applications. Owing to their ability to form solid solutions in a wide range of substituting atoms, perovskites are intensively explored as basic compositions to obtain materials with controlled properties. Series of low-loss perovskite system have been investigated and adjusted for microwave applications [1, 2]. However, the most widespread method for producing new materials is still an empirical one and slow progress is observed

[1] Author to whom any correspondence should be addressed.

in discovering and clarifying mechanisms controlling microwave dielectric parameters in complex systems. Correlations between structure and microwave dielectric characteristics of perovskite compounds have only been revealed for some particular compositions [3, 4]. Reaney *et al* [3] have established a relationship between the temperature coefficient of the related permittivity (τ_ε) and the structure tolerance factor for Ba- and Sr-based complex perovskites like $A^{2+}(B'_nB''_{1-n})O_3$ as well as their solid solutions. At the same time, the τ_ε behaviour in the solid solutions involving simple perovskites (ABO_3) does not obey the relationship. Wise *et al* [5] have attributed tuning of τ_f in microwave dielectrics to dilution of the average ionic polarizability and to the onset of an octahedral tilt transition above room temperature. Nevertheless, behaviour of microwave dielectric characteristics in solid solutions is generally difficult to predict, especially the compositional change of dielectric loss. Microwave loss in ceramics has known to be caused by both extrinsic factors (porosity, impurities, grain boundaries etc) and intrinsic ones (lattice absorption due to crystal anharmonicity) [6, 7]. Usually, the extrinsic contribution can be minimized using proper processing conditions. Change of lattice anharmonicity and associated dielectric loss in solid solutions depends on any crystal symmetry variation, namely a change of cell distortion, octahedral tilting, cation ordering etc. Thus there are too many factors affecting the behaviour of the Q-value.

Lanthanide-based complex perovskites were found to be of great interest as prospective microwave materials owing mainly to their high quality factor [8–12]. These perovskites have low tolerance factor because of considerable size misfit of constituting atoms and are characterized by an oxygen octahedral tilt, A-cation displacement and B-cation ordering [10, 11, 13]. Investigations of the materials suggest that the mentioned Reaney relationship [3] also seems to be valid for the $A^{3+}(B'_mB''_{1-m})O_3$ compositions, where A^{3+} is a lanthanide cation [14, 15]. In this family, the Mg/Ti 1:1 ordered monoclinic perovskites $La(Mg_{1/2}Ti_{1/2})O_3$ (LMT) and $Nd(Mg_{1/2}Ti_{1/2})O_3$ (NMT) have relative permittivity ∼26–27 in the gigahertz range and negative τ_f [11, 16]. The fact that the τ_f value of LMT is lower than that of NMT is in disagreement with what might be expected from the relations between τ_f and tolerance factor established by Reaney *et al* [3]. To clarify this contradiction, it has been decided to study the evolution of microwave dielectric properties in solid solutions of the LMT–NMT system. It was also of interest to study the change of the parameters ε', τ_f and Q in regard to A-site substitution without any other complicating factors.

The present work reports preparation and characterization of the $(1-x)$LMT–xNMT ceramics. Basic dielectric parameters (ε', τ_f and Q) were measured as a function of x in the gigahertz range. Compositional dependence of dielectric loss was analysed using the model of damped classical oscillators.

2. Experimental procedure

$(1-x)$LMT–xNMT ceramics ($x = 0$, 0.25, 0.5, 0.75 and 1) were prepared using powders obtained by a chemical route based on Pechini method, optimized previously for LMT [16]. In this procedure, the precursor resin was calcined at 750 °C for 3 h in order to obtain the powders with the required compositions. For all the compositions, the powders were isostatically pressed at 200 MPa and sintered at 1650 °C for 2 h in air with heating and cooling rates of 10 °C min^{-1}.

The sintered pellets were ground to obtain powders for x-ray diffraction (XRD) experiments. X-ray powder diffraction data were collected at room temperature using a Rigaku D/MAX-B diffractometer (Bragg–Brentano geometry, Cu Kα radiation, $2\theta = 15$–$115°$, step 0.02°, 7 s/step, graphite monochromator). Rietveld refinement was performed using GSAS suite [17].

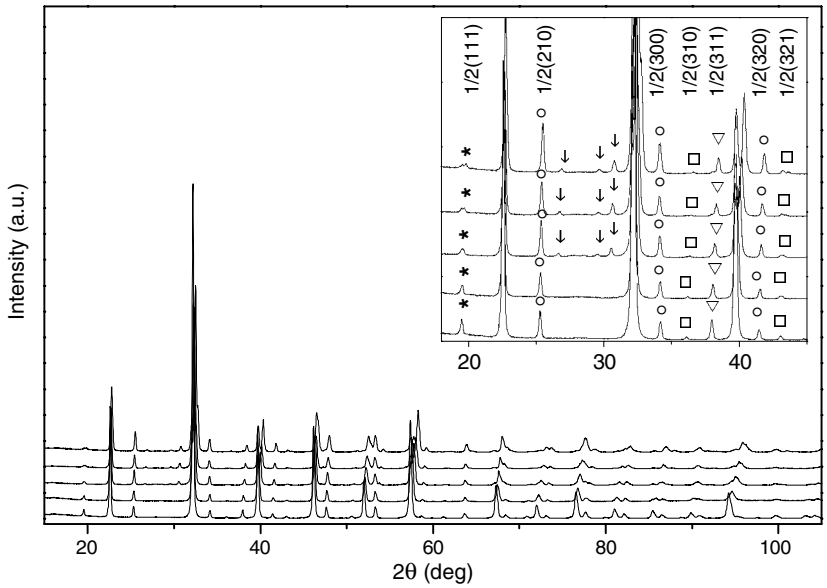

Figure 1. XRD patterns of $(1-x)$LMT–xNMT, $x = 0$ (bottom), 0.25, 0.5, 0.75 and 1.0 (top). The inset shows supercell reflections indicating Mg/Ti ordering ($\star$), antiparallel (La, Ba) displacement (O), in-phase octahedral tilting ($\square$), anti-phase octahedral tilting ($\triangledown$) and traces of Nd_2O_3 ($\downarrow$).

Relative density of sintered samples was determined from geometry and weight measurements and their microstructure was examined by scanning electron microscopy (SEM) (Hitachi S-4100). The samples for SEM observations were polished and thermally etched 50 °C below the sintering temperature for 2 min. Chemical homogeneity of the samples was confirmed by energy dispersive spectroscopy (EDS).

Measurements of dielectric properties at microwave frequencies were performed by the Hakki–Coleman method [18] at room temperature. τ_f was obtained by measuring the variation of resonant frequency (f) in an oxygen-free high-conductivity copper cavity, between -40 and +30 °C, while cooling at a rate of 2 °C min^{-1} (CTI Cryogenics model 22 refrigerator and 8200 cryocompressor with a Lakeshore 330 temperature controller) [19].

3. Results and discussion

As expected, since both compounds belong to the same space group, for the whole compositional range of the $(1-x)$LMT–xNMT system a solid solution can be formed (figure 1). XRD spectra of all the prepared compositions were successfully refined using the $P2_1/n$ space group. Traces of neodymium oxide (<2 wt%) were observed in the XRD patterns of the samples with $x = 0.5$, 0.75 and 1.0 (see arrows in the inset of figure 1).

In perovskite compounds, two mechanisms are commonly responsible for unit-cell doubling: cation ordering and tilting of oxygen octahedra. According to Glazer [20, 21], the superlattice reflections, with specific combinations of odd (o) and even (e) Miller indices, point to definite types of deviation of the structure from the undistorted cubic one, such as octahedral in-phase tilting (ooe, oeo, eoo), anti-phase tilting ($ooo, h+k+l > 3$), chemical ordering (ooo) and anti-parallel displacement of A-cations (eeo, eoe, oee). In the studied system all these features are present for all the compositions. That can be clearly observed in the inset of figure 1.

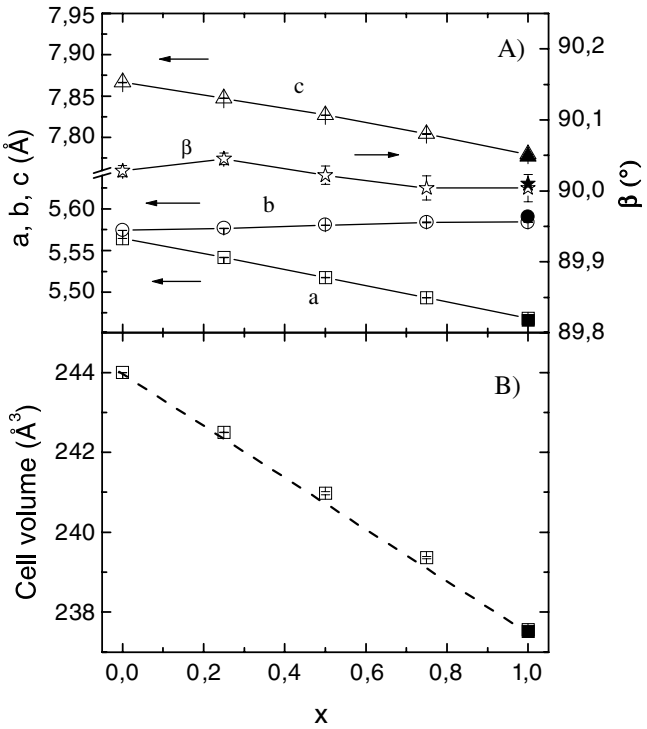

Figure 2. Cell parameters (A) and cell volume (B) as a function of Nd content (*a*—squares, *b*—circles, *c*—triangles, *β*—stars). Empty symbols—this work, filled—[22]. In the case of volume data error bars are smaller than symbols.

Figure 2(A) shows the cell parameter evolution as a function of neodymium content. A gradual decrease of *a* and *c* with the increase of Nd amount is observed, while the value of the *b* parameter is almost constant over the whole range. The parameters for NMT were found to be in very good agreement with those reported by Groen *et al* [22].

The cell volume gradually decreases with x according to the substitution of La^{3+} by the smaller Nd^{3+} (figure 2(B)). As seen, the dependence is slightly convex in comparison with the linear Vegard law (dashed line), supporting a random arrangement of the cations in the perovskite sublattice A. Actually, there is no driving force for ordering lanthanum and neodymium in the $(1-x)$LMT–xNMT system: these cations have equal oxidation state and are very close in size.

Figure 3 shows typical secondary electron SEM images of polished and thermally etched surfaces from samples of the $(1-x)$LMT–xNMT system ($x = 0$, 0.25, 0.5, 0.75 and 1). A dense and homogeneous microstructure without grains of secondary phases was observed. Furthermore, there is not a large variation of the grain size with composition.

Table 1 presents density and some microwave dielectric data for the ceramics of the studied system. Relative permittivity and temperature coefficient of resonant frequency obtained from dielectric measurements at microwave frequency range are plotted as a function of composition x in figures 4(A), (B). A small variation of these properties with the composition is observed.

The quality factor of the ceramics under study is expressed in terms of $Q \times f$. One can see in figure 4(C) that the $Q \times f$ dependence on composition is non-monotonic and exhibits a minimum value for $x = 0.5$. Since $Q \equiv 1/\tan\delta$ it means that dielectric loss is higher in the

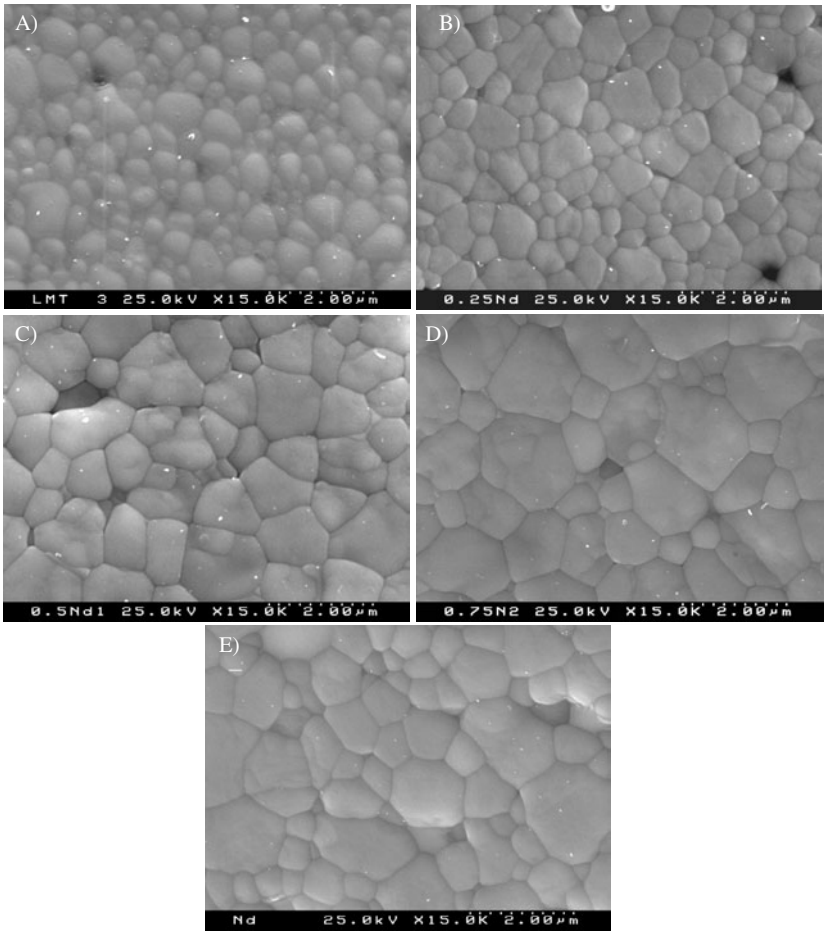

Figure 3. SEM images of polished and thermally etched surfaces of the $(1-x)$LMT–xNMT ceramics, where $x = 0$ (A), 0.25 (B), 0.5 (C), 0.75 (D) and 1 (E).

Table 1. Dielectric properties of the $(1-x)$LMT–xNMT ceramics in the microwave range.

x	Density (%)	ε	τ_f (ppm °C^{-1})	Q	f (GHz)
0.00	97.0	27.6	−81	16 110	7.10
0.25	96.3	27.9	−54	10 390	9.28
0.50	98.5	27.6	−48	4 550	9.12
0.75	97.9	26.7	−44	12 447	9.32
1.00	97.0	25.9	−47	16 160	9.36

middle of the system than in the end members. In our case the chemically prepared ceramics are apparently highly homogeneous in density (table 1) and grain size (figure 3). Hence the extrinsic contribution to dielectric loss of the $(1-x)$LMT–xNMT system is supposed to be independent of the composition x.

Regarding the intrinsic part of the loss, let us consider the responsible phonon absorption process, based on the widely used model of n damped classical oscillators [23]. According to the model the real (ε') and imaginary (ε'') parts of the complex permittivity ($\varepsilon^* = \varepsilon' + \mathrm{i}\varepsilon''$) are

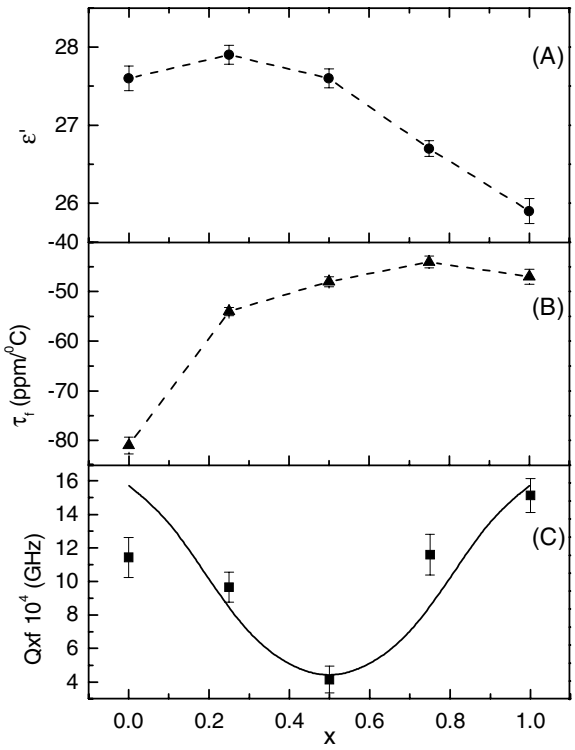

Figure 4. (A) Relative permittivity, (B) thermal coefficient of the resonant frequency and (C) $Q \times f$ value as a function of x for solid solutions $(1-x)$LMT–xNMT measured in the GHz range (solid curve—theoretical fit).

a function of circular frequency ($\omega = 2\pi f$) as follows:

$$\varepsilon'(\omega) = \varepsilon_\infty + \sum_{j=1}^{n} \frac{S_j(\omega_j^2 - \omega^2)}{(\omega_j^2 - \omega^2)^2 + \omega^2\gamma_j^2} \tag{1}$$

$$\varepsilon''(\omega) = \omega \sum_{j=1}^{n} \frac{S_j\gamma_j}{(\omega_j^2 - \omega^2)^2 + \omega^2\gamma_j^2}. \tag{2}$$

Here ε_∞ is the permittivity at 'infinitely high' frequencies; n is the number of infrared active polar modes; S_j, ω_j and γ_j are the strength, eigenfrequency and damping of the jth mode, respectively.

For monoclinic structure (space group $P2_1/n$, $Z = 4$) the factor group analysis [24] yields a number of IR active polar modes $n = 17$. From Kramers–Kronig analysis the existence of 15 active modes in LMT was experimentally estimated; two of them were extremely weak [25]. In comparison with the phonon spectrum of 1:1 ordered cubic perovskites of the $A(B'_{1/2}B''_{1/2})O_3$ series ($n = 4$) [6], the spectrum of any solid solution of the $(1-x)$LMT–xNMT system is very complex. However, four strongest modes related to fundamental vibrations also have to be present in the LMT monoclinic lattice. On increasing frequency these correspond to $A \leftrightarrow BO_6$ vibrations, $B–O_6$ stretching, $B'–B''$ stretching and BO_6 bending, respectively [6].

In the microwave range $\omega \gg \omega_j$, and then one can rewrite equations (1) and (2):

$$\varepsilon' \approx \varepsilon_\infty + \sum_{j=1}^{n} \frac{S_j}{\omega_j^2} \tag{3}$$

$$\varepsilon'' \approx \omega \sum_{j=1}^{n} \frac{S_j \gamma_j}{\omega_j^4}. \tag{4}$$

It has been generally accepted that the permittivity and loss in the microwave range are mainly determined by the contributions of the first two (low-frequency) modes [6]. The low-frequency polar soft mode is known to cause a great part of the intrinsic loss in displacive ferroelectrics [26]. In our case of non-ferroelectric perovskites the mode, being one of the strongest and lowest in frequency, should correspond to A $\leftrightarrow$ BO_6 vibrations [6]. Another significant contributor in microwave loss is the B–O_6 stretching mode. In the system under study, only the La/Nd substitution takes place and one can believe that the associated contribution is practically the same in each particular solid solution. Thus, the compositional behaviour of the microwave dielectric loss in the LMT–NMT system appears to be predominantly determined by the parameters (S, ω and γ) of the A $\leftrightarrow$ BO_6 vibration mode.

As seen from figures 4(C) and (A), the deviation in $Q \times f$ with x is about $\pm 40\%$ and only $\sim \pm 3\%$ in ε'. The change in eigenfrequency ($\Delta\omega = \omega - \omega_0$) of the vibration mode arising from substitution of one atom by another might be estimated using the expression for the local phonon mode [27]:

$$\omega^2 = \omega_0^2 \frac{M^2}{2MM' - M'^2}, \tag{5}$$

where M and M' are the weights of the host and substituting atom, respectively. Considering $M \equiv M_{\mathrm{Nd}}$ and $M' \equiv M_{\mathrm{La}}$, the relative change ($\Delta\omega/\omega_0$) is calculated to be less than 1%. Hence, the difference in the mode eigenfrequency due to the La/Nd substitution appears to be negligibly small. Taking into account the small variation of ε' with x one can assume that the effective strength S of the A $\leftrightarrow$ BO_6 vibration mode in the system is roughly constant (see equation (3). It should be recalled that only the first item in the sums of equations (3) and (4) is supposed to vary with composition. Since $Q \times f \sim \omega[\varepsilon'/\varepsilon'']$, it follows from equations (3) and (4) that the compositional variation of effective damping γ is responsible for the observed dependence of $Q \times f$ on x (figure 4(C)). Considering that in the $(1-x)$LMT–xNMT system so-called 'two-mode' behaviour [28] takes place, in the spectra of such solid solutions the peaks of both end members have to be present. Then the variable part of ε'' caused by La/Nd substitution might be represented according to equation (2) as

$$\varepsilon_1''(x) = \frac{\omega S_{\mathrm{La}} \gamma_{\mathrm{La}}}{(\omega_{\mathrm{La}}^2 - \omega^2)^2 + \omega^2 \gamma_{\mathrm{La}}^2} + \frac{\omega S_{\mathrm{Nd}} \gamma_{\mathrm{Nd}}}{(\omega_{\mathrm{Nd}}^2 - \omega^2)^2 + \omega^2 \gamma_{\mathrm{Nd}}^2}. \tag{6}$$

Figure 5 shows results of the $\varepsilon_1''(x)$ simulation with equation (6) using the real relative difference between ω_{La} and ω_{Nd}. Conditions of $S_{\mathrm{La}} = (1-x)S$ and $S_{\mathrm{Nd}} = xS$ (S = constant), $\gamma_{\mathrm{La}} = \gamma_{\mathrm{Nd}} \ll \omega_{\mathrm{La}}, \omega_{\mathrm{Nd}}$ were also assumed. The width of the resulting peak at half height is plotted in figure 6 as a function of x for certain γ values of the constituted modes. The ε'' peak width is known to be a measure of damping of the associated mode [23]. As the quality factor is inversely proportional to ε'', the obtained $\gamma(x)$ dependence of the effective damping might lead to $Q \times f$ compositional behaviour like that shown in figure 4(C) (solid curve).

The described decrease of $Q \times f$ in solid solutions in comparison with their end members seems to be common. However, other stronger effects usually appear to overlap this one.

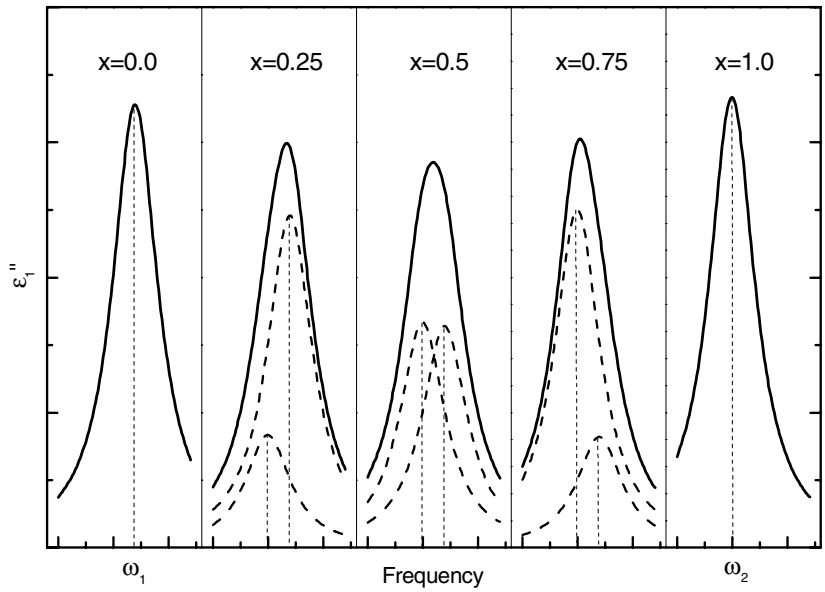

Figure 5. The resulting loss line profile as a sum of the lines corresponded to phonons with eigenfrequencies ω_1 and ω_2 ($\Delta\omega \ll \omega_1, \omega_2$) (equation (6)).

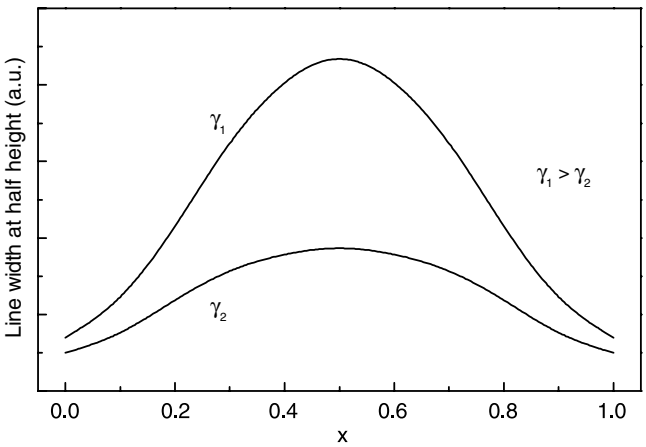

Figure 6. Width at half height of the resulting loss line simulated with equation (6) as a function of x at different dampings γ.

A number of microwave solid solutions have been formed through substitution of one atom by a set of others, like $A/(A'_mA''_{1-m})$ or $B/(B'_nB''_{1-n})$ [29]. Such substitutions are known to result in a noticeable modification of the phonon spectra and therefore the described effect becomes difficult to extract. Regarding solid solutions between complex perovskites, it has also been found that the compositional variation of crystal symmetry (as in system $Ba(Zn_{1/3}Nb_{2/3})O_3$–$Sr(Zn_{1/3}Nb_{2/3})O_3$ [30]) as well as a change in degree and/or type of cation ordering (e.g. $Ba(Mg_{1/3}Ta_{2/3})O_3$–$La(Mg_{2/3}Ta_{1/3})O_3$) [15] strongly affect the quality factor. In the LMT–NMT solid solutions the $Q \times f$ compositional behaviour described above could be more obvious because neither heterovalent atomic substitution nor structure and ordering change take place simultaneously in the system.

4. Conclusions

Powder processing by a chemical route allowed preparation of dense and homogeneous ceramics in the whole compositional range of the system $(1-x)La(Mg_{1/2}Ti_{1/2})O_3$–$xNd(Mg_{1/2}Ti_{1/2})O_3$. Rietveld refinement of all the compositions was performed using the $P2_1/n$ space group describing A-cation displacement and both phase and antiphase octahedral tilt as well as Mg/Ti ordering. No compositional transformation of the structure was observed in the system. A monotonic change of cell parameters was detected to exist in the whole range of solid solutions.

The relative permittivity and temperature coefficient of the resonant frequency measured at microwave frequencies as a function of x showed rather non-linear dependence. $Q \times f$ in this system was found to be a non-monotonic function of x. Its value decreases in solid solutions in comparison with their end members. Since all the studied ceramics were well processed, the extrinsic part of the microwave loss has been considered to be minimal and independent of composition. The main contributor to dielectric loss is therefore one of the first and strongest modes corresponding to $A \leftrightarrow BO_6$ vibrations, which is changed by La/Nd substitution. The observed compositional dependence of the loss (and, thereby, $Q \times f$) has been described qualitatively with the damped classical oscillator model. The 'two-mode' behaviour of the $A \leftrightarrow BO_6$ vibration mode in the solid solutions has been assumed. Effective damping of the resulting mode was calculated to be larger in the middle of the system than in the end members. As the microwave loss is determined by the damping and the former is inversely proportional to quality factor, this corresponded to the compositional behaviour of $Q \times f$ observed in the system investigated.

Acknowledgment

The authors acknowledge the Foundation for Science and Technology (FCT-Portugal) for their support.

References

[1] Cava R J 2001 *J. Mater. Chem.* **11** 54
[2] Wersing W 1991 *Electronic Ceramics* (London: Elsevier) pp 67–119
[3] Reaney I M, Colla E L and Setter N 1994 *Japan. J. Appl. Phys.* **33** 3984
[4] Cho S Y, Kim I T and Hong K S 1999 *J. Mater. Res.* **14** 114
[5] Wise P L, Reaney I M, Lee W E, Iddles D M, Cannell D S and Price T J 2002 *J. Mater. Res.* **17** 2033
[6] Zurmuhlen R, Petzelt J, Kamba S, Voitsekhovski V V, Colla E and Setter N 1995 *J. Appl. Phys.* **77** 5341
[7] Petzelt J and Setter N 1993 *Ferroelectrics* **150** 89
[8] Kucheiko S, Kim H J, Yeo D H and Jung H J 1996 *Japan. J. Appl. Phys.* **35** 668
[9] Cho S Y, Ko K H, Hong K S and Park S J 1997 *J. Korean Ceram. Soc.* **34** 330
[10] Youn H J, Kim I T, Hong K S and Kim H 1997 *Ferroelectrics* **193** 167
[11] Cho S Y, Kim C H, Kim D W, Hong K S and Kim J H 1999 *J. Mater. Res.* **14** 2484
[12] Paik J H, Choi C H, Nahm S, Byun J D and Lee H J 1999 *J. Mater. Sci. Lett.* **18** 889
[13] Lee D Y, Yoon S J, Yeo J H, Nahm S, Paik J H, Whang K C and Ahn B G 2000 *J. Mater. Sci. Lett.* **19** 131
[14] Akbas M A and Davies P K 1998 *J. Am. Ceram. Soc.* **81** 2205
[15] Youn H J, Hong K S, Kim H and Kim H 1998 *J. Korean Phys. Soc.* **32** S524
[16] Seabra M P and Ferreira V M 2002 *Mater. Res. Bull.* **37** 255
[17] Larson A C and Von Dreele R B 1987 *Los Alamos National Laboratory Report* LAUR-86-748
[18] Hakki B W and Coleman P D 1960 *IRE Trans. Microw. Theory Techniques* **8** 402
[19] Kajfez D and Guillion P 1986 *Dielectric Resonators* (Zurich: Artech)
[20] Glazer A M 1972 *Acta Crystallogr.* B **28** 3384
[21] Glazer A M 1975 *Acta Crystallogr.* A **31** 756

[22] Groen W A, van Berkel F P F and Ijdo D J W 1986 *Acta Crystallogr.* C **42** 1472
[23] Petzelt J, Pacesova S, Fousek J, Kamba S, Zelezny V, Koukal V, Schwarzbach J, Gorshunov B P, Kozlov G V and Volkov A A 1989 *Ferroelectrics* **93** 77
[24] Rousseau D L, Bauman R P and Porto S P S 1981 *J. Raman Spectrosc.* **10** 253
[25] Seabra M P, Salak A N, Ferreira V M, Vieira L G and Ribeiro J L 2003 *Ferroelectrics* at press
[26] Gurevich V L and Tagantsev A K 1991 *Adv. Phys.* **40** 719
[27] Kittel C 1986 *Introduction to Solid State Physics* (New York: Wiley)
[28] White B W 1974 *Infrared Spectra of Minerals* (London: Mineral Soc.) pp 87–110
[29] Akbas M A and Davies P K 1998 *J. Am. Ceram. Soc.* **81** 670
[30] Kim J S, Lee J H, Lim Y S, Jang J W and Kim I T 1997 *Japan. J. Appl. Phys.* **36** 5558